Bulletin of Entomological Research

cambridge.org/ber

Transcriptome analysis reveals the role of Zelda in the regulation of embryonic and wing development of *Tribolium castaneum*

Shanshan Gao[1], Shuang Xue[1], Tian Gao[1], Ruixue Lu[1], Xinyi Zhang[1], Yonglei Zhang[2], Kunpeng Zhang[1] and Ruimin Li[1]

[1]Department of Food and Bioengineering, Anyang Institute of Technology, Anyang, Henan 455000, China and [2]College of Life Sciences, Nanjing Normal University, Nanjing, Jiangsu 210023, China

Research Paper

Cite this article: Gao S, Xue S, Gao T, Lu R, Zhang X, Zhang Y, Zhang K, Li R (2023). Transcriptome analysis reveals the role of Zelda in the regulation of embryonic and wing development of *Tribolium castaneum*. *Bulletin of Entomological Research* **113**, 587–597. https://doi.org/10.1017/S0007485323000263

Received: 4 October 2022
Revised: 12 June 2023
Accepted: 12 June 2023
First published online: 21 July 2023

Keywords:
embryonic development; physiological function; RNAi; *Tribolium castaneum*; Zelda

Corresponding author:
Kunpeng Zhang;
Email: zhangkunpengag@163.com;
Ruimin Li;
Email: liruimin920130@163.com

Abstract

Zinc finger protein (Zelda) of *Tribolium castaneum* (*TcZelda*) has been showed to play pivotal roles in embryonic development and metamorphosis. However, the regulatory mechanism of *TcZelda* associated with these physiology processes is unclear. Herein, the developmental expression profile showed that *Zelda* of *T. castaneum* was highly expressed in early eggs. Tissue expression profiling revealed that *TcZelda* was mainly expressed in the larval head and adult ovary of late adults and late larvae. *TcZelda* knockdown led to a 95% mortality rate in adults. These results suggested that *TcZelda* is related to the activation of the zygote genome in early embryonic development. Furthermore, 592 differentially expressed genes were identified from the ds*Zelda* treated group. Compared with the control group, *altered disjunction* (*ALD*) and *AGAP005368-PA* (*GAP*) in the ds*Zelda* group were significantly down-regulated, while *TGF-beta, propeptide* (*TGF*) was significantly up-regulated, suggesting that *TcZelda* may be involved in insect embryonic development. In addition, the expression of *Ubx ultrabithorax* (*UBX*), *Cx cephalothorax* (*CX*), *En engrailed* (*EN*), and two *Endocuticle structural glycoprotein sgabd* (*ABD*) genes were significantly down-regulated, suggesting that they may cooperate with *TcZelda* to regulate the development of insect wings. Additionally, *Elongation* (*ELO*), *fatty acid synthase* (*FAS*), and *fatty acyl-CoA desaturase* (*FAD*) expression was inhibited in ds*Zelda* insects, which could disturb the lipase signaling pathways, thus, disrupting the insect reproductive system and pheromone synthesis. These results may help reveal the function of *TcZelda* in insects and the role of certain genes in the gene regulatory network and provide new ideas for the prevention and control of *T. castaneum*.

Introduction

Insects are the only invertebrates with the ability to fly. Their wings are not only the core structure of flight but also play an important role in orientation, protection, communication, and courtship (Shyy *et al.*, 2016). For a long time, the molecular mechanism of insect wing development has been an area of particular interest. Holometabolous insects need to undergo four developmental stages to become adults (Rolff *et al.*, 2019). Previous studies have shown that some genes are involved in the early development of *Drosophila* wings. These genes include transcription factors, such as engrailed (en), serum response factor (SRF) (Simmonds *et al.*, 1998), apterous (ap) (Bourgouin *et al.*, 1992), scalloped (sd) (Celniker and Rubin, 2003), and vestigial (vg) (Williams *et al.*, 1994). Studies have shown that *BGIBMGA000319* gene encodes Cys2-His2 (C2H2) zinc finger protein, which is homologous to B lymphocyte maturation induction protein-1 (*BLIMP-1*) gene (Wu *et al.*, 2019). *BMBLIMP-1* of silkworm has been specifically up-regulated during metamorphosis and has been highly expressed in the wings of the pupa on the third day of the pupal stage, and RNA interference (RNAi) has led to wing abnormalities (Wu *et al.*, 2019). Because *BMBLIMP-1* is a C2H2 zinc finger gene, it may be related to the development of silkworm pupa wings.

Zinc finger protein is a type of transcription factors with a finger domain, playing an important role in gene expression regulation, cell differentiation, embryonic development, apoptosis, and other important life processes. In 1985, the zinc finger structure was first discovered in the transcription factor TFIIIA of *Xenopus laevis* (Miller *et al.*, 1985). The structure of zinc finger protein is defined as the existence of several Cys residues in an amino acid sequence of the regulatory protein, which is a zinc-dependent DNA-binding domain forming a short and stable finger-like structure by binding Zn^{2+} for self-folding (Frankel and Pabo, 1988). Since then, researchers have found a large number of proteins containing zinc finger structure, collectively known as zinc finger proteins. According to the conserved motif characteristics of the zinc finger, Berg and Shi (1996) divided zinc finger proteins into nine categories: C2H2 (Cys2His2), C8 (Cys8), C6 (Cys6), ring type (Cys3HisCys4), Cys2HisCys,

Lim type (Cys2HisCys5), C4 (Cys4), and Cys3His. Multiple types of zinc finger proteins may also be expressed in the same tissue (Miller *et al.*, 1985). Zinc fingers protein can bind not only DNA and RNA, but also DNA–RNA hybrid double-strand molecules and other zinc finger proteins or themselves to regulate gene expression at the transcriptional and translational levels (Zhao and Zhao, 2009).

The different expression patterns of *BgZelda* in *Blattella germanica* seem to be related to metamorphosis (Ventos-Alfonso *et al.*, 2019). Holometabolous species, such as *Drosophila melanogaster*, produce larvae different from those of adults during embryogenesis. Therefore, in addition to MZT, the expression of *Zelda* in *D. melanogaster* may activate the continuous gene set needed to establish the morphology of vermicular larvae during embryogenesis (Ventos-Alfonso *et al.*, 2019). The *Zelda* gene is also expressed in later stage embryonic development of *Apis mellifera*, which is related to the development of precursor cells of the central nervous system (Pires *et al.*, 2016). Other studies have found that *Zelda* is continuously expressed during embryonic development, including the developing central nervous system and trachea (Pearson *et al.*, 2012). Additionally, it was reported that 55 and 58 *CCCH* zinc finger protein genes were identified in humans and mice, respectively. *CCCH* genes are expressed at different levels in all tissues. They are highly expressed in tissues with high energy consumption, such as the heart, muscle, blood vessels, and brown adipose tissue (Liang *et al.*, 2008*b*).

Zinc finger transcription factor Zelda (also known as vielfaltig) plays an important role in the transition from the mother cell to the zygotic cell (MZT) in *D. melanogaster*. In *D. melanogaster*, mutant embryos lacking Zelda have defects in the cell germ formation and cannot activate genes necessary for cell formation, sex determination, and pattern formation (Liang *et al.*, 2008*a*; Schulz *et al.*, 2015). Moreover, Zelda studied in this paper is an important factor regulating early gene expression and plays a key role in the activation of the early zygotic genome of *D. melanogaster* (Liang *et al.*, 2008*a*). *T. castaneum* is a holometabolous insect with short embryonic development, and *Zelda* also plays a key role in the posterior division and configuration of *T. castaneum* adult disk structure (Dönitz *et al.*, 2015; Ribeiro *et al.*, 2017; Ventos-Alfonso *et al.*, 2019). However, regulatory network about how *TcZelda* performs these functions in insects is still unclear. To further explore the signaling systems of *TcZelda* involved in insect physiology, RNA sequencing and RNA interference were combined to study the potential function of *TcZelda* in *T. castaneum*. The results will shed a new light into molecular regulatory mechanisms of other relative genes in *T. castaneum*.

Material and methods

Experimental samples

T. castaneum Georgia-1 (GA-1) strain was used for all experiments. It was placed in a flask with a mass ratio of flour to yeast powder at 19:1 and cultured in an artificial climate box with a set temperature of 30°C and a humidity of 40% (Begum *et al.*, 2009).

Expression profiling of TcZelda gene

The tissue (head, antennae, ovary, testis, epidermis, midgut, and fat body) were dissected from 100 10-day-old adults and eight developmental stages were extracted by Trizol method. The eight stages of development included early eggs (1 day old, ~50 mg), late eggs (3 days old, ~50 mg), early larvae (1 day old, 3 individuals), late larvae (15 days old, 3 individuals), early pupae (1 day old, 3 individuals), late pupae (5 days old, 3 individuals), early adults (1 day old, 3 individuals), and late adults (10 days old, 3 individuals). Finally, the extracted RNA was reversed into circular DNA (cDNA) by reverse transcriptional reagents 4× gDNA wiper Mix and 5× HiScript Q RT Supermix II. Quantitative reverse transcription polymerase chain reaction (qRT-PCR) was used to analyze cDNA in different developmental stages and tissues. The reaction system consisted of 0.25 μl forward and backward primers (10 μM), 2 × 5 μl AceQ Universal SYBR qPCR Master Mix, 3.5 μl ddH_2O, and 1 μl cDNA. Three technical and biological repeats were performed for each group of samples, and the melting curve was analyzed to ensure that only one PCR product was amplified.

Synthesis and injection of dsRNA

dsRNA of *TcZelda* and *VER* (*T. castaneum* vermillion, GenBank AY052390) was synthesized with primers designed by Primer Premier 5.0. The gene primers are shown in table S1. The promoter of T7 polymerase was added to the 5' end of two forward primers, and dsRNA was then synthesized by TranscriptAi T7 high yield transcription kit. Using Nanoject III instruments (Drummond Scientific, Philadelphia, USA), the obtained dsRNA (200 ng/150 nl) was injected into the body cavity of each larva (15 days old), and the same volume of dsVER or injection buffer (IB) was microinjected as negative control and blank control, respectively. In each experiment, 30–40 larvae were injected, and the biological repeats were performed three times. The larvae injected with dsRNA were cultured normally, and the survival rate was recorded on the fourth day. Three individuals of each group were collected on day 4 after dsRNA injection to examine the knockdown level of the targeted gene by qRT-PCR.

Images of adults were taken using a Zeiss SteREO Discovery V8 (Zeiss, Oberkochen, Germany) stereomicroscope. ZEN2.3 microscope software (Blue edition, Zeiss) was used to control the microscope, image acquisition, and exportation of TIFF files. The images were processed using Photoshop CS6 software (Adobe Systems Inc., San Jose, CA, USA) for converting RAW format to EPS format, which then were compatible with the Adobe Illustrator version 6.0 software (Adobe Systems Inc.) vector graphics image editor program.

Extraction and sequencing of total RNA

Six samples, including two control and two ds*Zelda*-treated samples harvested on the fourth day after dsRNA injection (each sample contained six larvae), were selected for RNA-Seq analysis. The concentration and purity of RNA were detected by Nanodrop2000/2000c. Only RNA with A260/A280 > 1.80 was used for the follow-up study, and the integrity of RNA was detected by Agilent 2100 Bioanalyzer. The reverse transcription was then performed with 1000 ng of total RNA (A260/A280 ratio >1.8 and A260/A230 ratio >2.0) using HiScript II reverse transcriptase (Vazyme, Nanjing, China), following the manufacturer's manual. Samples of RNA with established purity and integrity were sequenced at Beijing Genomics Institute (Shenzhen, China) on the BGISEQ-500 platform. The sequences were deposited at the National Center for Biotechnology Information (NCBI) database under accession numbers

https://doi.org/10.1017/S0007485323000263 Published online by Cambridge University Press

SAMN28580502 and SAMN28580503 for IB samples and SAMN2857338 and SAMN2857338 for ds*Zelda* samples.

Filtering and mapping of RNA-Seq data

The original sequencing data contained reads with low quality, joint contamination, and high unknown base N content. These reads needed to be removed before data analysis to ensure the reliability of the results. SOAPnuke, a BGI-developed filtering software, was used for statistical analysis, while Trimmomatic was used for filtering. Specific steps included the removal of the reads containing the joint (joint contamination), the removal of the reads with an unknown base N content greater than 5%, and the removal of low-quality reads (defined as the reads with a mass value <15 that represented >20% of the total base number of the reads). The resulting clean reads were aligned with the reference genome sequence using HISAT (Kim *et al.*, 2015) and with the reference gene sequences using Bowtie2 (Li and Dewey, 2011; Langmead and Salzberg, 2012).

Differential gene expression analysis

To authenticate differentially expressed genes (DEGs) in the treated and control samples, RPKM values (reads per kilobase per million mapped reads) were used to calculate gene expression levels, and DEGs were defined as genes with $|\log2 - (T/C)| \geq 0.5$ and adjusted *P*-values of <0.05 based on DEseq2. DEGs were analyzed by hierarchical clustering using the heatmap function in R software. Furthermore, functional analysis and annotation of DEGs in *T. castaneum* were performed using the Gene Ontology (GO) database, which included molecular functions, cellular components, and biological processes, and the Kyoto Encyclopedia of Genes and Genomes (KEGG) database.

Validating RNA-sequencing data by qRT-PCR

On the fourth day after dsRNA injection, the total RNA was extracted from six larvae of ds*Zelda* or control groups, and two biological replicates were carried out for each sample. Total RNA of larval samples in the control and ds*Zelda* groups was extracted by RNAiso^{TM}Plus (TaKaRa), and then 1 μg of total RNA was reverse transcribed to synthesize the first strand of cDNA. RNA-sequencing data were verified by qRT-PCR according to the instructions of FastStart SYBR Green Master (Roche). *Tcrps3* (GenBank accession number was XM_965494) was used as the internal reference gene (Horn and Panfilio, 2016), and the gene expression was analyzed by the $2^{-\Delta\Delta CT}$ method (Livak and Schmittgen, 2001). The experiment was biologically repeated at least three times. The gene primers are shown in table S1.

Statistical analysis

Gene expression was calculated by the $2^{-\Delta\Delta CT}$ method (Livak and Schmittgen, 2001), and the gene expression data, the mean values obtained for the RNAi-treated larvae, and the mean values obtained for the control larvae were compared by one-way analysis of variance in combination with Fisher's least significant difference multiple comparison test using SPSS version 13.0 (SPSS Inc., Chicago, IL, USA). All data were presented as the mean ± standard error (SE). The error bars represented SEs among three biological replications. *P*-values of <0.05 were regarded as statistically significant, and *P*-values of <0.001 were considered extremely significant.

Results

Developmental stage and tissue-specific expression profile of TcZelda

The qRT-PCR results revealed that transcripts of *TcZelda* were detected at all stages from embryo to adult and strongly expressed at the early egg stage (fig. 1a). The expression of *TcZelda* in different tissues of larvae and adults was further studied. In the larval tissue, compared with the whole larva, the expression of *TcZelda* was the most significant in the head, followed by the epidermis, fat body, hemolymph, and the intestine, where it was the lowest (fig. 1b). In adult tissues, compared with whole adult beetles, the expression of *TcZelda* was the most significant in the ovary, followed by fat body, head and epidermis, and very low in the gut, antennae, testis, and accessory glands (fig. 1c).

Observation of biological characterization after RNAi

TcZelda gene was silenced by RNAi to further determine the function of *TcZelda* in insects. After injection on the third day, the silence efficiency of *TcZelda* was measured by qRT-PCR, and the transcript levels of *TcZelda* were reduced by about 70% as compared to control (fig. 2a). We counted the mortality rate after RNAi, of which the mortality rate of insects injected with IB was 9%, that of insects injected with ds*VER* was 9.5%, and that of insects injected with ds*Zelda* was 95% (fig. 2b). In addition, the death state of adults included the inability of wings to close, shortening of the antennae, and possible fusion of the ankles of the legs (fig. 2c).

Transcriptome profiling by RNA sequencing

The transcriptional group was sequenced, and 84.20 million clean reads were obtained from the control group and ds*Zelda*-treated samples. Each sample has a clean reading of about 40 million, which is enough for quantitative analysis of gene expression. In the sequencing analysis, the control group produced 42.64 million raw reads, while the treatment group produced 43.82 million raw reads, of which about 96% passed the CleanReadsQ20 (table 1). The ratio of clean reads to raw reads of the four gene libraries was between 97.24 and 97.71%. The SOAPaligner/SOAP2 software was used to compare the sequenced readings from these sequences with the reference genome database of *T. castaneum*. In total, 85.24% of the control reads could match the genome, of which 47.37% had only one match with the genome, while 86.29% of the ds*Zelda* groups readings could match the genome, and the only matching proportion in the genome was 48.39% (table 1). About 15% of the reads in the two gene libraries did not match the reference genome. The Pearson correlation coefficients of all gene expressions between every two samples were calculated and reflected in the form of a heat map to reflect the correlation of gene expression between samples. The correlation coefficient can reflect the similarity of overall gene expression among samples. The higher the correlation coefficient is, the more similar is the gene expression level (fig. S1). In sum, these data suggest that the two biological replicates were highly correlated for both the control and treated samples.

Functional analysis of DEGs based on RNA-seq data

Fragments per kilobase million (FPKM) values of unigenes from the control and treatment groups with knockdown target gene

https://doi.org/10.1017/S0007485323000263 Published online by Cambridge University Press

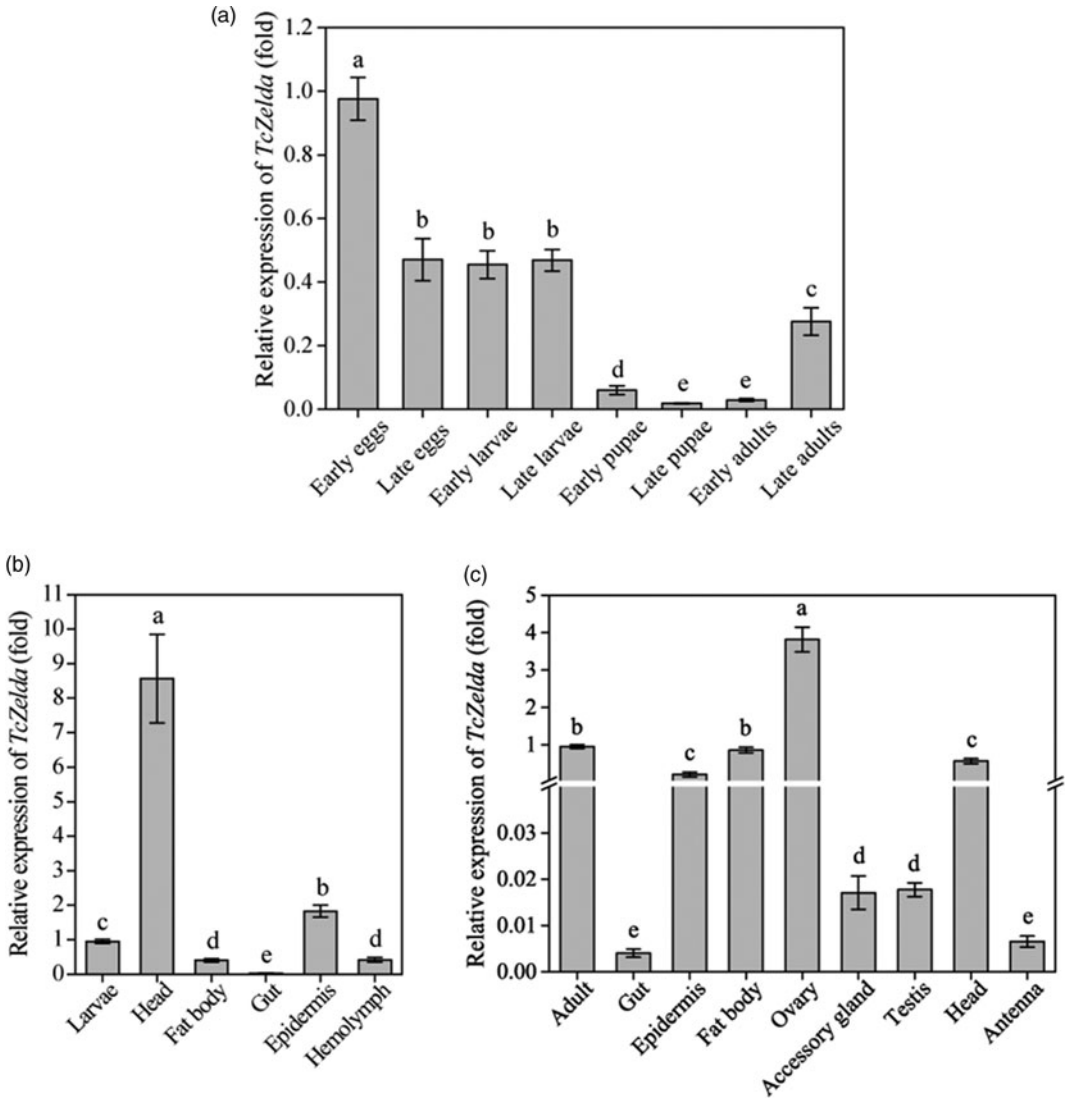

Figure 1. Expression of *TcZelda* gene in the developmental stage (A), different tissues of larvae (B) and adults (C) of *T. castaneum*. Early egg (1 day old), late egg (3 days old), early larva (1 day old), late larva (20 days old), early pupa (1 day old), late pupa (5 days old), early adult (1 day old), and late adult (10 days old). Different letters on the column chart indicate that there are significant differences in different developmental stages. Late larvae (15 days old) and adults were dissected under the somatotype microscope, including the whole larva, head integument, fat body, gut, and hemolymph. Additionally, the whole adult, head, integument, fat body, gut, ovary, antennae, testis, and accessory gland were dissected. The transcriptional level of *Tczelda* in the whole larva and adult was used to calibrate the tissue-specific expression profile. The vertical line is the standard error of the mean ($n = 3$), and the vertical line letters indicate that the mean expression values at different developmental stages are significantly different at $P < 0.05$.

were compared to further explore the function of *TcZelda* in *T. castaneum*. A total of 592 DEGs were identified, including 277 up-regulated genes and 315 down-regulated genes (fig. 3a, table S2). The cluster heat map of differential gene expression showed the similarity and difference of DEGs expression levels of two biological repeats from the control and ds*Zelda* groups (fig. 3b). Ten genes (5 up-regulated genes and 5 down-regulated genes) were randomly selected and evaluated by qRT-PCR to further verify the accuracy of transcriptome data and DEGs results (table S1). The randomly selected DEGs in qRT-PCR and transcriptome data (fig. 3c) had a similar adjustment trend, indicating that the data of RNA-seq was reliable.

To annotate these DEGs, we performed a GO functional analysis (fig. 4, table S3). Gene Ontology can be divided into three functional categories: molecular function, cellular component, and biological process. According to the functional classification of differential genes, 592 differential genes (DEGs) were divided into 9, 3, and 17 main functional groups, respectively. Cellular anatomical entity (GO:0110165) with 322 genes (54.39%) and binding (GO:0005488) with 235 genes (39.70%) are the major biological processes. Cellular (GO:0009987) and metabolic processes (GO:0008152), containing 201 genes (33.95%) and 130 genes (21.96%), were dominant in the main categories of biological process, respectively. Additionally, GO term enrichment analysis showed that DEGs were associated with 30 GO terms (table S3), and the most enriched GO terms were oxidoreductase activity (GO:0016491), developmental process (GO:0032502), anatomical structure development (GO:0048856), and multicellular organism development (GO:0007275) (fig. S2). Further, KEGG enrichment analysis showed that there were 20 pathways significantly enriched in DEGs compared with the whole transcriptome background with a Q value of ≤ 0.05, and the most

https://doi.org/10.1017/S0007485323000263 Published online by Cambridge University Press

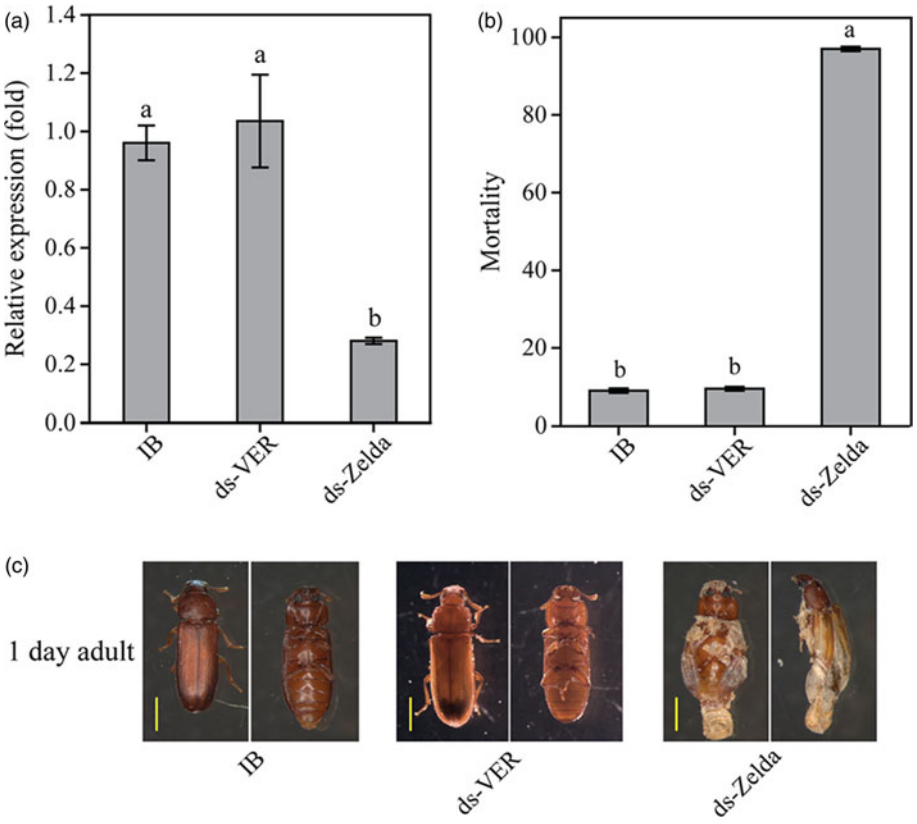

Figure 2. The ds*Zelda*-mediated suppression of *TcZelda* transcripts as determined by qRT-PCR (a). Mortality rate of the beetles after larval RNAi (b) phenotype (c). The insects in the control group were injected with the same amount of IB or ds*VER*. The error bar represents the standard error of three biological repeats. The letters at the top of the bar chart indicate that there are significant differences at a level of P of <0.05 between different treatment groups. Mortality statistics of 4 days after injection of IB, dsVER, or dsZelda (b). The data in the figure are the mean ± standard error (nasty 3). Different letters on the column chart indicate that there are significant differences among different treatments at $P < 0.05$ level (scale bars: 1000 μm for panel C).

enriched pathways were lysosome (ko04142), protein digestion and absorption (ko04974), and focal adhesion (ko04510) (fig. 5, tables S4, S5)

Genes related to embryonic development, wing development, and fatty acid metabolism

In these DEGs databases, there were six genes related to embryonic development, including *altered disjunction* (*ALD*), *TGF-beta*, *propeptide* (*TGF*), *AGAP005368-PA* (*GAP*), and genes encoding cilia- and flagella-associated protein 44, advillin, and condensing complex subunit 1 (table 2). Additionally, nine DEGs were involved in the development of insect wings (table 3), and 11 DEGs were involved in the fatty acid metabolism of insects (table 4). *Ubx ultrabithorax* (*UBX*), *Cx cephalothorax* (*CX*), *optomotor-blind-like* (*OMB*), and five *Endocuticle structural glycoprotein sgabd* (*ABD*) genes were involved in the development of insect wings (table 3). The proteins involved in fatty acid metabolism included delta-12 desaturase, elongation of very long-chain fatty acids protein AAEL008004, fatty acid synthase, and palmitoyl-protein thioesterase 1 (table 4).

Discussion

Previous studies have shown that *Zelda* is expressed during MZT in *D. melanogaster* and *T. castaneum*. In these species, *Zelda* even plays a role in the post-embryonic development. This *Zelda* function beyond the range of MZT might be related to the evolution and innovation of holometabolous insects. The expression of *Zelda* related to blastoderm and gastrula formation has been observed in the early embryonic development of western honeybees (Pires *et al*., 2016), indicating that *Zelda* plays the same role as the activator of the early zygotic genome described in *D. melanogaster* (Liang *et al*., 2008*a*; Ventos-Alfonso *et al*., 2019).

Table 1. Summary statistics of read numbers based on the *T. castaneum* transcriptome

	Control		ds*Zelda*	
	Control_1	Control_2	ds*Zelda*_1	ds*Zelda*_2
Total raw reads (M)	43.82	41.46	43.82	43.82
Total clean reads (M)	42.61	40.32	42.65	42.82
Clean reads Q20 (%)	95.55	95.91	95.84	95.87
Clean reads ratio (%)	97.24	97.24	97.32	97.71
Total mapping (%)	84.05	86.42	86.15	86.42
Uniquely mapping (%)	45.67	49.06	48.47	48.31

https://doi.org/10.1017/S0007485323000263 Published online by Cambridge University Press

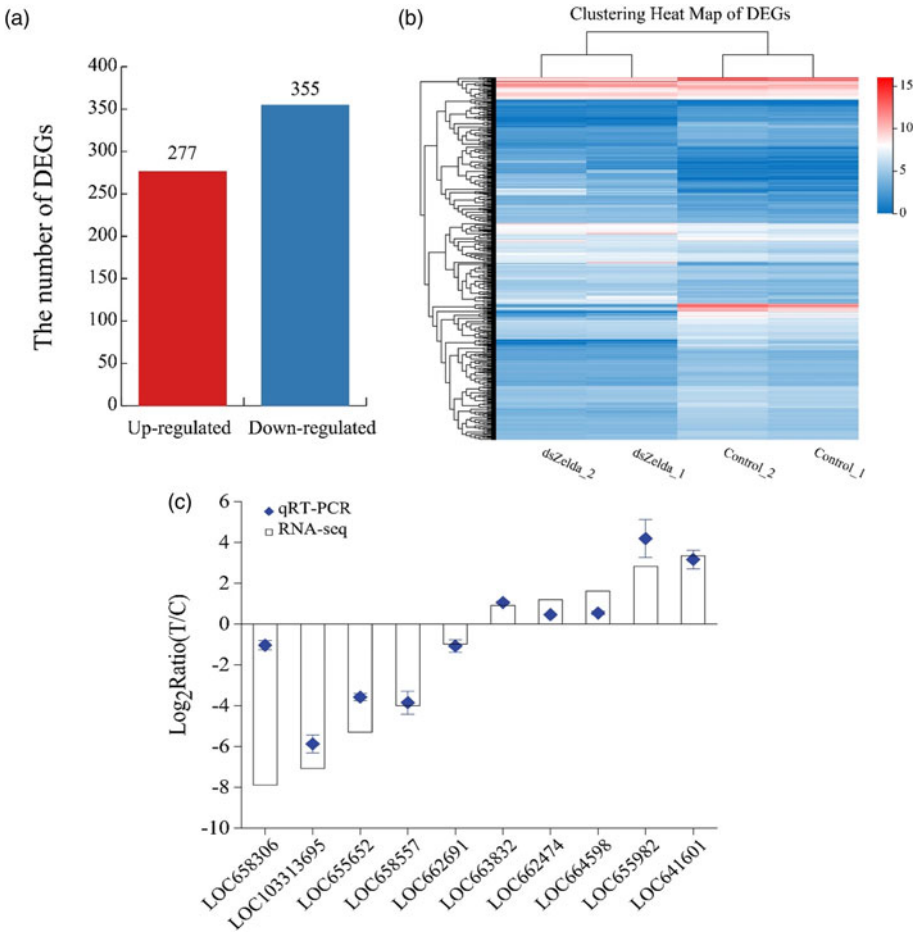

Figure 3. Analysis of differential gene expression after *TcZelda* gene knockdown. The number of differential genes (a) and differential gene expression clustering heat map (b) between the ds*Zelda* and control groups. Comparison of gene expression profiles between RNA sequencing and qRT-PCR detection (c). The row represents a single gene, and the column represents the comparison of genes between the ds*Zelda* treatment and control groups. The FPKM of the sample obeys standard normal distribution. The column on the right clusters the samples ($N = 6$) based on the similarity of Log2 (FPKM + 1). Group C was the control group, and group T was the ds*Zelda* treatment group.

Our results showed that *TcZelda* was expressed in eight key developmental stages (fig. 1a), indicating that *TcZelda* may be involved in various physiological processes. *TcZelda* highly expressed in embryos and larvae, then decreased expression in pupae, and slightly increased expression in late adults. It is speculated that *TcZelda* gene plays a key role in the activation of the early zygotic genome and late embryonic development. Through the analysis of our experimental results, *TcZelda* was mainly highly expressed in the head of larvae (fig. 1b), and it is speculated that *TcZelda* may be involved in the development of precursor cells in the central nervous system. It was found that *TcZelda* was also expressed in the epidermis, fat body, and hemolymph (fig. 1c); thus, we

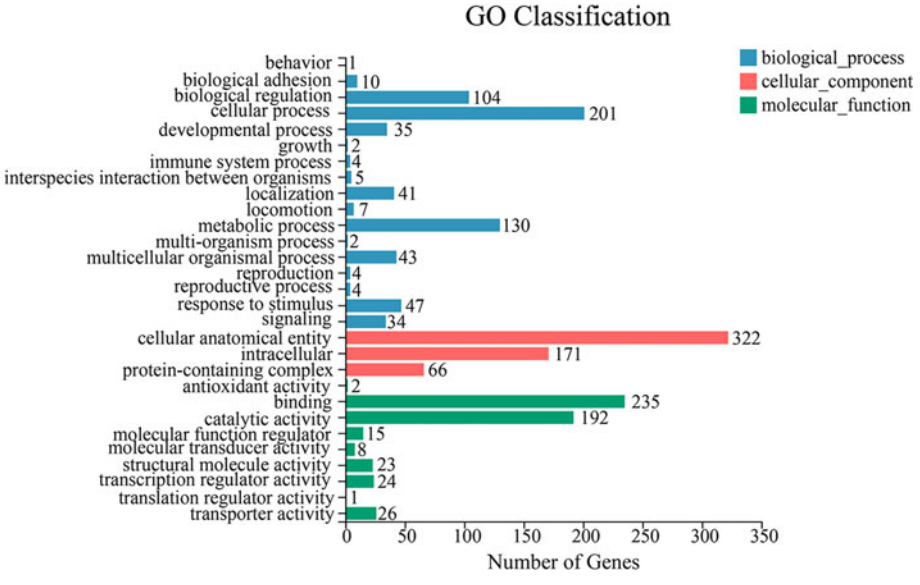

Figure 4. GO analyses of DEGs in ds*Zelda* and control samples. Different colors represent GO categories. The *x*-axis shows the number of DEGs. The *y*-axis shows the GO terms.

https://doi.org/10.1017/S0007485323000263 Published online by Cambridge University Press

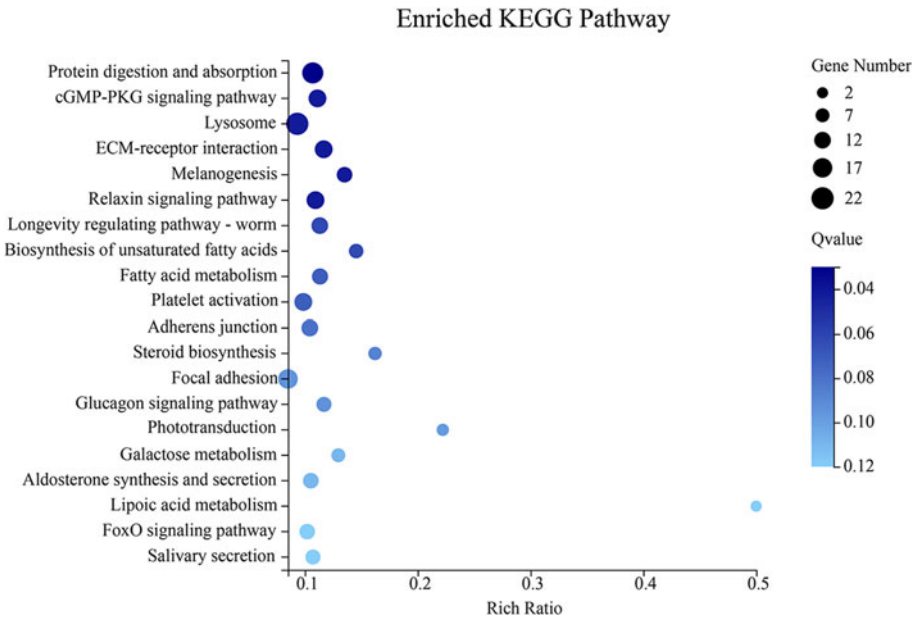

Figure 5. KEGG pathway analyses of DEGs in ds*Zelda* and control samples. Pathway significance is shown together with the *Q*-value (color), rich factor (vertical ordinate), and the number of genes (size of circles).

speculated that *TcZelda* gene might be involved in the regulation of fatty acid metabolism. The results showed that the expression of *TcZelda* in the ovary was the highest in adult tissues (fig. 1c), and the gene was probably related to the activation of the zygotic genome during the transition from mother cell to zygotic cell in early embryonic development.

Keratin and chitin are the main components of the insect exoskeleton and play an important role in wing development (Iconomidou *et al.*, 2005). By analyzing the experimental results, it was found that *TcZelda* was expressed in the exoskeleton of adults (fig. 1c). Thus, *TcZelda* may play an important role in providing the stability of the stratum corneum during wing development. Moreover, *TcZelda* was expressed in the head and fat body (fig. 1B). It is speculated that *TcZelda* may also be involved in the metabolism of fatty acids in larval tissue. Additionally, the analysis of the experimental results showed that the expression and function of *TcZelda* significantly exceeded that of embryos in all metamorphosis species (fig. 1A), which was proved by its role in the disk structure formation of adults (Ribeiro *et al.*, 2017) and neuroblasts in *D. melanogaster* larvae (Reichardt *et al.*, 2018). Studies have shown that *Zelda* gene expression in *D. melanogaster* and *T. castaneum* extends to the middle and late stages of embryonic development, which may be a factor leading to the total metamorphosis innovation of the semi-abnormal ancestors of endoptera insects (Ventos-Alfonso *et al.*, 2019).

This study suppressed the expression of *TcZelda* gene by using RNAi. Four days after the injection of ds*Zelda*, qualitative analysis was performed with RT-PCR, and then interference efficiency was quantitatively analyzed with qPCR. Compared with the control group, the expression of *TcZelda* was significantly down-regulated, and the interference efficiency was about 70% (fig. 2A). After the expression of *TcZelda* gene was suppressed, the mortality rates at different developmental stages were statistically analyzed. The cumulative mortality rate of the treatment group injected with ds*Zelda* was 97%, including 72% in the pupa stage and 23% in the adult stage (fig. 2B). Therefore, we speculate that *TcZelda* might play an important role in the physiological and biochemical response of *T. castaneum* pupal stage. After the expression of the gene was suppressed, through the observation and analysis of adult biological characteristics, it was found

Table 2. Genes involved in reproductive process

Gene ID	Protein	Log2 ratio(T/C)	Regulation (T/C)	*P*-value	Phenotype after RNAi of DEGs in *T. castaneum*[a]
LOC662564	Altered disjunction(ald)	−0.86	Down	1.50E-03	/
LOC663146	Cilia- and flagella-associated protein 44	1.27	Up	7.97E-11	/
LOC663549	Advillin	−1.49	Down	1.72E-07	10.0%[b]
LOC664135	Condensin complex subunit 1	−1.08	Down	1.12E-03	100.0%[b]
LOC660630	AGAP010211-PA-like protein(gap)	−1.07	Down	3.88E-04	/
LOC100142362	AGAP005368-PA(gap)	2.12	Up	1.36E-03	/
LOC660239	TGF-beta, propeptide(TGF)	1.42	Up	2.43E-04	/

C, control; T, ds*Zelda*.
[a]Metamorphosis and survival after RNAi were analyzed (https://ibeetle-base.uni-goettingen.de/).
[b]Lethalities 11 days after larval injection (includes death as larva, prepupa, pupa).

https://doi.org/10.1017/S0007485323000263 Published online by Cambridge University Press

Table 3. Genes involved in the development of insect wings

Gene ID	Protein	Log2 Ratio(T/C)	Regulation (T/C)	*P*-value	Phenotype after RNAi of DEGs in T. castaneum[a]
LOC641535	Ubx ultrabithorax	−0.59	Down	8.85E-05	/
LOC641551	En engrailed	−0.77	Down	1.44E-05	10%[b]
LOC641600	Cx cephalothorax	−1.08	Down	1.23E-06	100.0%[b], 30.0–50.0% embryo/egg with embryonic tissue, no cuticle[c], 70.0% elytra duplicated[d]
LOC661159	Optomotor-blind-like	−0.67	Down	2.11E-03	40.0%[b]
LOC657808	Endocuticle structural glycoprotein sgabd-8	2.37	Up	1.09E-04	/
LOC658557	Endocuticle structural glycoprotein sgabd-1	−4.00	Down	7.21E-17	30.0%[b]
LOC659176	Endocuticle structural glycoprotein sgabd-5	2.65	Up	2.98E-05	/
LOC662771	Endocuticle structural glycoprotein sgabd-2	−2.81	Down	1.73E-10	/
LOC657728	Endocuticle structural glycoprotein sgabd-4	2.24	Up	2.13E-03	/

C, control; T, ds*Zelda*.
[a]Metamorphosis and survival after RNAi were analyzed (https://ibeetle-base.uni-goettingen.de/).
[b]Lethalities 11 days after larval injection (includes death as larva, prepupa, pupa).
[c]13 days after female pupal injection.
[d]16 days after larval injection.

that the wings of the adults were not closed, the antennae were shortened, the reproductive leaves of females were reduced, and the tarsal joints of the two legs were fused (fig. 2c), indicating that *TcZelda* also plays a key role in the posterior segmentation and configuration of the adult disk structure of the whole metamorphosis species with short embryonic development (Ventos-Alfonso *et al*., 2019). However, in the course of the experiment, due to the death of a large number of pupae after RNAi, a small number of adults with successful eclosion had a wide gap between male and female insects; hence, it was difficult to perform phenotypic and reproductive statistics of the next generation. Therefore, the experiment needs further exploration.

By inhibiting the expression of *vielfaltig* gene (also known as *Zelda*) by RNAi technology, it can inhibit the growth of the stratum corneum in the egg stage, decrease the fecundity of larvae after injection, and die in the pupal stage, which is consistent with the results of iBeetle-Base (Dönitz *et al*., 2015). Thus, *Zelda* plays a key role in the embryonic development, wing development, and fatty acid metabolism of insects. We used an IlluminaHisSeq2000 for RNA sequencing to fully understand the role of *Zelda* gene in reproductive development and pupa lethality in *T. castaneum*. After *TcZelda* gene knockdown, according to the functional annotation of the gene, 592 DEGs were assigned to 29 major functional groups (fig. 4, table S3), and 20 pathways were significantly rich in DEGs (fig. 5, table S4), of which 277 and 355 DEGs were up-regulated and down-regulated (fig. 3c, table S2), respectively. These results provide a basic understanding for the study of the role of *Zelda* gene in the functional regulation system of *T. castaneum*.

Table 4. Genes involved in fatty acid metabolism

Gene ID (NCBI)	Protein	Log2 ratio(T/C)	Regulation (T/C)	*P*-value
LOC100233160	Delta-12 desaturase	1.50	Up	5.54E-04
LOC103314796	Acyl-coa Delta (11) desaturase	0.90	Up	6.03E-06
LOC103315088	Elongation of very long-chain fatty acids protein 7-like	1.65	Up	4.42E-04
LOC655561	Elongation of very long-chain fatty acids protein	−0.53	Down	2.31E-03
LOC656313	Acyl-coa Delta (11) desaturase	0.83	Up	2.21E-03
LOC657543	Short/branched chain-specific acyl-coa dehydrogenase, mitochondrial	−0.89	Down	2.17E-06
LOC658084	Palmitoyl-protein thioesterase 1	0.84	Up	1.82E-04
LOC659322	Acyl-coa Delta (11) desaturase	4.05	Up	2.27E-08
LOC660113	Fatty acid synthase	−1.44	Down	1.35E-04
LOC660385	Peroxisomal acyl-coenzyme A oxidase 3	0.50	Up	1.49E-03
LOC662823	Elongation of very long-chain fatty acids protein AAEL008004	−6.82	Down	3.94E-33

C, control; T, ds*Zelda*.

https://doi.org/10.1017/S0007485323000263 Published online by Cambridge University Press

Zinc finger protein *Zelda* plays a key role in the activation of the insect's early zygotic genome. Six genes, including *GAP*, *TGF*, and *ALD*, were found by comparing the control group with the ds*Zelda* group (table 2). *Altered disjunction* (*ALD*) is a magnetic-specific meiotic mutation-related protein. Studies have shown that the gene product of *ALD* plays a role in preventing the exchange of X chromosome and fourth chromosome in non-homologous segregation events (O'Tousa, 1982). It can be concluded that *ALD* is a key gene in the insect reproductive system. *GAP* genes can limit the region of the somatic segment of the embryo, and the mutation of these genes can change the number or polarity of the somatic structure (Boos *et al*., 2018). Gene products of *GAP* divide embryos into regions equivalent to three body segments. Additionally, products of spacer genes form concentration gradients in their respective expression regions, and the location information provided by these gradients is transmitted to downstream genes, which orderly regulate the formation of embryonic development patterns and finally determine the boundaries between body segments and the fate of cells in different parts of the embryo (Sánchez and Thieffry, 2001). After *TcZelda* was knocked down, the expression of *ALD* and *GAP* was down-regulated, which indicating that *Zelda* and *ALD* and *GAP* might be upstream and downstream genes in the reproductive regulatory system, respectively.

The *TGFβ* superfamily is composed of a class of polypeptide growth factors related to the structure and function of different tissues, including *TGFβ*, *activin*, *inhibin*, and *BMP* (Li *et al*., 2018). Members of the *TGFβ* family exist widely in various tissues of many organisms and play an important role in the development of organisms and organs. Reproductive stem cells in *Drosophila* ovary are known to be regulated by the Dpp signaling. The gene related to the survival of early male germ cells is *DPP*, and the gene related to the proliferation and differentiation of early male germ cells is *BAM*. Studies have shown that *TGFβ* signal transduction may affect the expression of these genes, regulating the proliferation and differentiation of germ cells (Chen and McKearin, 2003; Song *et al*., 2004). After *TcZelda* knockdown, the expression of *TcZeldaβ* was up-regulated, indicating that the gene may complement the function of *TcZelda*. The above results confirmed that *TGFβ* was involved in insect embryonic development, which was consistent with the results of the previous tissue expression profile.

There were some genes related to the development of insect wings. As the only and earliest winged group of invertebrates, the flying ability of insects allows them to have great advantages in migration, foraging, and courtship (Guo *et al*., 2017). Some studies have shown that the expression of *UBX* and *ABD-A* is suppressed by RNAi. There are 20 sheath-wing discs in ten body segments from the middle chest to the 8th ventral segment (T2–T8), which is the same as that of *Drosophila*. *UBX* is used to distinguish the front and rear wings, except that in the hind wings, *UBX* forms membrane wings by inhibiting the specific genes of the sheath wing, such as stratum corneum thickening genes, and the hind wings are specialized into sheath wings after being knocked out (Tomoyasu *et al*., 2005). As a copy of *SCR*, the loss of function of *Cephalo-thorax* (*CX*) can lead to the formation of additional tissue similar to the sheath wing structure in the forechest (T1) (Guo *et al*., 2017). After the injection of dsRNA of *TcZelda*, the expression of *UBX* and *ABD* genes decreased, while among the five *ABD* genes, the expression of *ABD-8*, *ABD-5*, and *ABD-4* was significantly up-regulated, and that of *ABD-1* and *ABD-2* was significantly down-regulated (table 3). Therefore, we speculate that the function of *TcZelda* gene is similar to that of these genes, this is supported by the fact that it is also similar to the results of the early development stage and tissue expression profile. *TcZelda* plays an important role in the development of insect wings.

As mentioned above, we found that *TcZelda* is also expressed in the epidermis, fat body, and hemolymph; hence, we speculate that *TcZelda* gene may be involved in the regulation of fatty acid metabolism. In the KEGG enrichment pathway, there were also 11 DEGs related to insect fatty acid metabolism, including *ELO*, *FAD*, and *FAS* (table 4). *FAS* was located in the cytoplasm and can catalyze the reaction of acetyl-CoA with malonic acyl-CoA, while palmitic acid can be obtained by the reddest reaction (Jakobsson *et al*., 2006). The study of *FAS* in insects focused on spatiotemporal expression and function and its effect on insect diapause. Some studies have shown that RNAi with *FAS* can reduce the content of *FAS* and fecundity in the ovary of brown planthopper (Lei *et al*., 2016). After RNA interferes with *FAS-1* and *FAS-3* of female mosquitoes, female mosquitoes cannot store lipids needed for winter; therefore, these two *FAS* play an important role in fat storage in the early diapause stage (Sim and Denlinger, 2009). *ELO* is the rate-limiting condensase obtained in the first step of the fatty acid extension reaction (Leonard *et al*., 2004). The study of *ELO* in insects has focused on *Drosophila melanogaster*, including the effect of *ELO* on reproductive function and the role of *ELO* in pheromone synthesis and the function of the epidermis. Some studies have shown that directional RNA interferes with *NOA* (ELO^{CG3971}) in the late developmental stage of *Drosophila* testis germ cells, which can lead to male *Drosophila* infertility. Moreover, *NOA* damages the motor function of *D. melanogaster* and significantly reduces its survivability (Jung *et al*., 2007).

FAD is an enzyme that can catalyze the formation of double bonds on specific sites of fatty acyl-CoA. Acyl-CoA Delta-11 desaturase belong to intact membrane proteins and is a type of fatty acyl-CoA desaturase (*FAD*) (Haritos *et al*., 2014). *FAD* of insect has been widely studied, mainly focusing on the role of *FAD* in pheromone synthesis. By feeding *FAD* inhibitor CAY10566 to *Drosophila*, Wang *et al*. reduced the unsaturated fatty acids and slowed down the growth of *Drosophila*. After the first molting, the expression of ecdysone regulatory protein was no longer induced, normal molting could not take place, and the insect died a few days later (Wang *et al*., 2016). Additionally, *FAD* at different sites can also affect the diversity of insect pheromones (Albre *et al*., 2012). At the same time, 56 genes were down-regulated in *TcZedla* knockdown beetles, and these genes could lead to impaired embryonic development of insects, suggesting that *TcZedla* gene may regulate embryonic development of *TcZedla* through these genes in *T. castaneum* (table S5). The up-regulation or down-regulation of DEGs expression also indicates that *TcZelda* may have similar functions, which further confirms the important role of *TcZelda* in embryonic development and reproduction and provides clues for the high expression of *TcZelda* in the epidermis, fat body, and hemolymph. Still, the specific mechanism needs to be further studied.

Conclusion

There were 592 DEGs between ds-*TcZelda* and control insects. These results suggest that *TcZelda* may not only regulate insect embryonic development through *ALD*, *GAP*, and *TGF* genes but also participate in insect wing development through *UBX*, *CX*,

https://doi.org/10.1017/S0007485323000263 Published online by Cambridge University Press

and *ABD*. Additionally, the knockdown of *TcZelda* gene led to significantly different expression of genes, such as *FAS*, *ELO*, and *FAD*, which are involved in fatty acid metabolism, might be related to the high expression of *TcZelda* in insect head, epidermis, fat body, and hemolymph, and might be involved in insect reproduction and pheromone synthesis. These results may help to find new pest target genes and more suitable methods for pest control.

Supplementary material. The supplementary material for this article can be found at https://doi.org/10.1017/S0007485323000263.

Financial support. This study was sponsored by the Staring Foundation for the Doctor, Anyang Institute of Technology (grant number BSJ2019009, BSJ2019022 and BSJ2021040); the Staring Foundation of Innovation and Practice Base for Postdoctors, Anyang Institute of Technology (grant numbers BHJ2020008); the Scientific and Technological Project of Henan Province (grant number 212102110444).

Competing interest. None.

References

Albre J, Liénard MA, Sirey TM, Schmidt S, Tooman LK, Carraher C, Greenwood DR, Löfstedt C and Newcomb RD (2012) Sex pheromone evolution is associated with differential regulation of the same desaturase gene in two genera of leafroller moths. *PLoS Genetics* **8**, e1002489.

Begum K, Li B, Beeman RW and Park Y (2009) Functions of ion transport peptide and ion transport peptide-like in the red flour beetle *Tribolium castaneum*. *Insect Biochemistry and Molecular Biology* **39**, 717–725.

Berg JM and Shi Y (1996) The galvanization of biology: a growing appreciation for the roles of zinc. *Science* **271**, 1081–1085.

Boos A, Distler J, Rudolf H, Klingler M and El-Sherif E (2018) A re-inducible gap gene cascade patterns the anterior-posterior axis of insects in a threshold-free fashion. *Elife* **7**, e41208.

Bourgouin C, Lundgren SE and Thomas JB (1992) Apterous is a *Drosophila* LIM domain gene required for the development of a subset of embryonic muscles. *Neuron* **9**, 549–561.

Celniker SE and Rubin GM (2003) The *Drosophila melanogaster* genome. *Annual Review of Genomics and Human Genetics* **4**, 89–117.

Chen D and McKearin D (2003) Dpp signaling silences bam transcription directly to establish asymmetric divisions of germline stem cells. *Current Biology* **13**, 1786–1791.

Dönitz J, Schmitt-Engel C, Grossmann D, Gerischer L, Tech M, Schoppmeier M, Klingler M and Bucher G (2015) iBeetle-Base: a database for RNAi phenotypes in the red flour beetle *Tribolium castaneum*. *Nucleic Acids Research* **43**, D720–D725.

Frankel AD and Pabo CO (1988) Fingering too many proteins. *Cell* **53**, 675.

Guo S, Dan L, Li Z, Jie S and Entomology DO (2017) Present status and perspectives of the researches on insect wing development. *Journal of Plant Protection* **44**, 185–195.

Haritos VS, Horne I, Damcevski K, Glover K and Gibb N (2014) Unexpected functional diversity in the fatty acid desaturases of the flour beetle *Tribolium castaneum* and identification of key residues determining activity. *Insect Biochemistry and Molecular Biology* **51**, 62–70.

Horn T and Panfilio KA (2016) Novel functions for Dorsocross in epithelial morphogenesis in the beetle *Tribolium castaneum*. *Development* **143**, 3002–3011.

Iconomidou VA, Willis JH and Hamodrakas SJ (2005) Unique features of the structural model of 'hard' cuticle proteins: implications for chitin-protein interactions and cross-linking in cuticle. *Insect Biochemistry and Molecular Biology* **35**, 553–560.

Jakobsson A, Westerberg R and Jacobsson A (2006) Fatty acid elongases in mammals: their regulation and roles in metabolism. *Progress in Lipid Research* **45**, 237–249.

Jung A, Hollmann M and Schäfer MA (2007) The fatty acid elongase NOA is necessary for viability and has a somatic role in *Drosophila* sperm development. *Journal of Cell Science* **120**, 2924–2934.

Kim D, Langmead B and Salzberg SL (2015) HISAT: a fast spliced aligner with low memory requirements. *Nature Methods* **12**, 357–360.

Langmead B and Salzberg SL (2012) Fast gapped-read alignment with Bowtie 2. *Nature Methods* **9**, 357–359.

Lei L, Jiang Y, Liu Z, You L and Wu J (2016) Jinggangmycin increases fecundity of the brown planthopper, Nilaparvata lugens (Stål) via fatty acid synthase gene expression. *Journal of Proteomics* **130**, 140.

Leonard AE, Pereira SL, Sprecher H and Huang YS (2004) Elongation of long-chain fatty acids. *Progress in Lipid Research* **43**, 36–54.

Li B and Dewey CN (2011) RSEM: accurate transcript quantification from RNA-Seq data with or without a reference genome. *BMC Bioinformatics* **12**, 323.

Li HY, Lin XW, Geng SL and Xu WH (2018) TGF-β and BMP signals regulate insect diapause through Smad1-POU-TFAM pathway. *Biochim Biophys Acta Mol Cell Res* **1865**, 1239–1249.

Liang HL, Nien CY, Liu HY, Metzstein MM, Kirov N and Rushlow C (2008*a*) The zinc-finger protein Zelda is a key activator of the early zygotic genome in *Drosophila*. *Nature* **456**, 400–403.

Liang J, Song W, Tromp G, Kolattukudy PE and Fu M (2008*b*) Genome-wide survey and expression profiling of CCCH-zinc finger family reveals a functional module in macrophage activation. *PLoS ONE* **3**, e2880.

Livak KJ and Schmittgen TD (2001) Analysis of relative gene expression data using real-time quantitative PCR and the 2(-Delta Delta C(T)) Method. *Methods* **25**, 402–408.

Miller J, McLachlan AD and Klug A (1985) Repetitive zinc-binding domains in the protein transcription factor IIIA from Xenopus oocytes. *EMBO Journal* **4**, 1609–1614.

O'Tousa J (1982) Meiotic chromosome behavior influenced by mutation-altered disjunction in *Drosophila melanogaster* females. *Genetics* **102**, 503–524.

Pearson JC, Watson JD and Crews ST (2012) *Drosophila melanogaster* Zelda and single-minded collaborate to regulate an evolutionarily dynamic CNS midline cell enhancer. *Developmental Biology* **366**, 420–432.

Pires CV, Freitas FC, Cristino AS, Dearden PK and Simões ZL (2016) Transcriptome analysis of honeybee (*Apis mellifera*) haploid and diploid embryos reveals early zygotic transcription during cleavage. *PLoS ONE* **11**, e0146447.

Reichardt I, Bonnay F, Steinmann V, Loedige I, Burkard TR, Meister G and Knoblich JA (2018) The tumor suppressor Brat controls neuronal stem cell lineages by inhibiting Deadpan and Zelda. *EMBO Reports* **19**, 102–117.

Ribeiro L, Tobias-Santos V, Santos D, Antunes F, Feltran G, de Souza Menezes J, Aravind L, Venancio TM and Nunes da Fonseca R (2017) Evolution and multiple roles of the Pancrustacea specific transcription factor zelda in insects. *PLoS Genetics* **13**, e1006868.

Rolff J, Johnston PR and Reynolds S (2019) Complete metamorphosis of insects. *Philosophical Transactions of the Royal Society of London B Biological Sciences* **374**, 20190063.

Sánchez L and Thieffry D (2001) A logical analysis of the *Drosophila* gap-gene system. *Journal of Theoretical Biology* **211**, 115–141.

Schulz KN, Bondra ER, Moshe A, Villalta JE, Lieb JD, Kaplan T, McKay DJ and Harrison MM (2015) Zelda is differentially required for chromatin accessibility, transcription factor binding, and gene expression in the early *Drosophila* embryo. *Genome Research* **25**, 1715–1726.

Shyy W, Kang CK, Chirarattananon P, Ravi S and Liu H (2016) Aerodynamics, sensing and control of insect-scale flapping-wing flight. *Proceedings. Mathematical, Physical, and Engineering Sciences/the Royal Society* **472**, 20150712.

Sim C and Denlinger DL (2009) Transcription profiling and regulation of fat metabolism genes in diapausing adults of the mosquito *Culex pipiens*. *Physiological Genomics* **39**, 202–209.

Simmonds AJ, Liu X, Soanes KH, Krause HM, Irvine KD and Bell JB (1998) Molecular interactions between vestigial and scalloped promote wing formation in *Drosophila*. *Genes & Development* **12**, 3815–3820.

Song X, Wong MD, Kawase E, Xi R, Ding BC, McCarthy JJ and Xie T (2004) Bmp signals from niche cells directly repress transcription of a differentiation-promoting gene, bag of marbles, in germline stem cells in the *Drosophila* ovary. *Development* **131**, 1353–1364.

Tomoyasu Y, Wheeler SR and Denell RE (2005) Ultrabithorax is required for membranous wing identity in the beetle *Tribolium castaneum*. *Nature* **433**, 643–647.

Ventos-Alfonso A, Ylla G and Belles X (2019) Zelda and the maternal-to-zygotic transition in cockroaches. *FEBS Journal* **286**, 3206–3221.

Wang Y, da Cruz TC, Pulfemuller A, Grégoire S, Ferveur JF and Moussian B (2016) Inhibition of fatty acid desaturases in *Drosophila melanogaster* larvae blocks feeding and developmental progression. *Archives of Insect Biochemistry and Physiology* **92**, 6–23.

Williams JA, Paddock SW, Vorwerk K and Carroll SB (1994) Organization of wing formation and induction of a wing-patterning gene at the dorsal/ventral compartment boundary. *Nature* **368**, 299–305.

Wu SY, Tong XL, Li CL, Ding X, Zhang ZL, Fang CY, Tan D, Hu H, Liu H and Dai FY (2019) BmBlimp-1 gene encoding a C2H2 zinc finger protein is required for wing development in the silkworm *Bombyx mori*. *International Journal of Biological Sciences* **15**, 2664–2675.

Zhao N and Zhao F (2009) Advances in research on zinc finger protein. *Letters in Biotechnology* **20**, 131–134.

https://doi.org/10.1017/S0007485323000263 Published online by Cambridge University Press